Electronic Supplementary Material (ESI) for Dalton Transactions.

Fabrication of $Co@SiO_2@C/Ni$ submicrorattles as Highly Efficient catalysts for 4-nitrophenol reduction

Xiaohui Guo[a], Min Zhang*[a], Jing Zheng[a], Jingli Xu[a], Tasawar Hayat[b], Njud S. Alharbi[c], Baojuan Xi [d], and Shenglin Xiong*[d]

[a]College of Chemistry and Chemical Engineering, Shanghai University of Engineering Science, Shanghai 201620, PR China Email: zhangmin@sues.edu.cn

[b]Department of Mathematics, Quaid-I-Azam University, Islamabad 44000, Pakistan NAAM Research Group, King Abdulaziz University, Jeddah, Saudi Arabia

[c]Biotechnology Research Group, Department of Biological Sciences, Faculty of Science, King Abdulaziz University, Jeddah, Saudi Arabia

[d] Key Laboratory of the Colloid and Interface Chemistry, Ministry of Education, and School of Chemistry and Chemical Engineering, Shandong University, Jinan, 250100, PR China. E-mail: chexsl@sdu.edu.cn

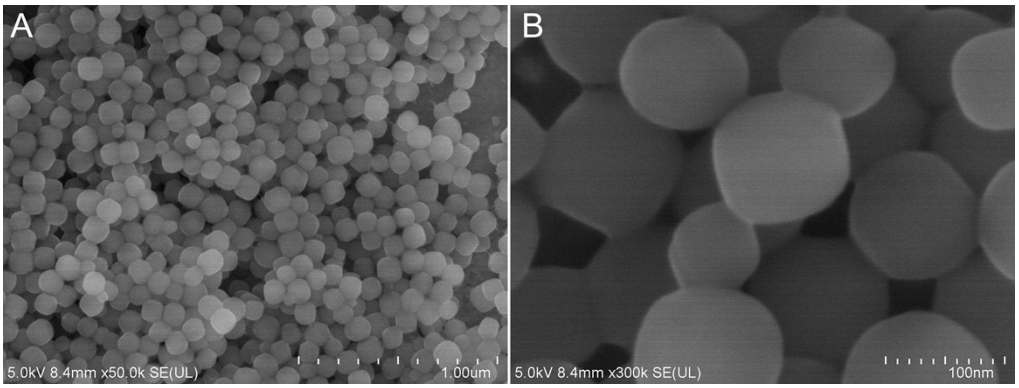

Figure S1. SEM images of $Co_3[Co(CN)_6]_2$ cubes with different magnification

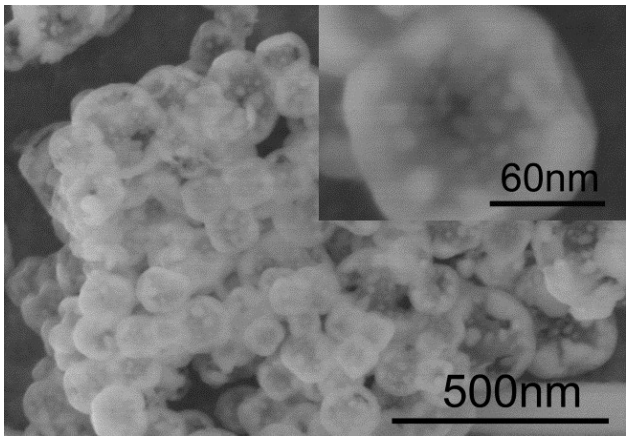

Figure S2. SEM images of Co@SiO_2-500 submicrorattles.

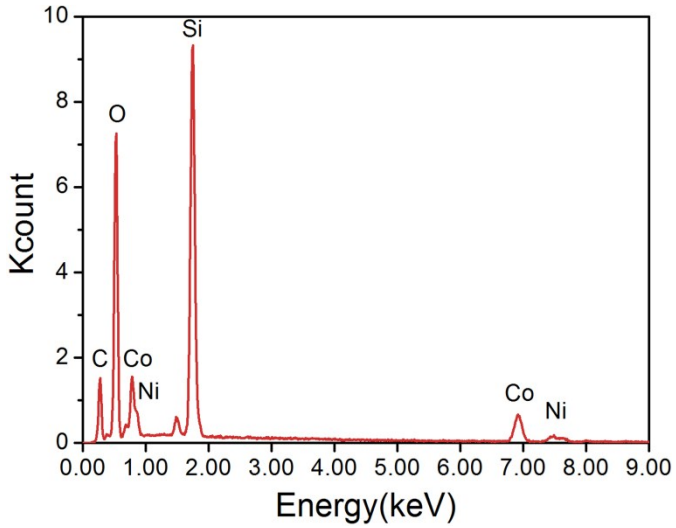

Figure S3. Energy-disperse X-ray spectrum (EDS) of Co@SiO_2@C/Ni-500 submicrorattles.

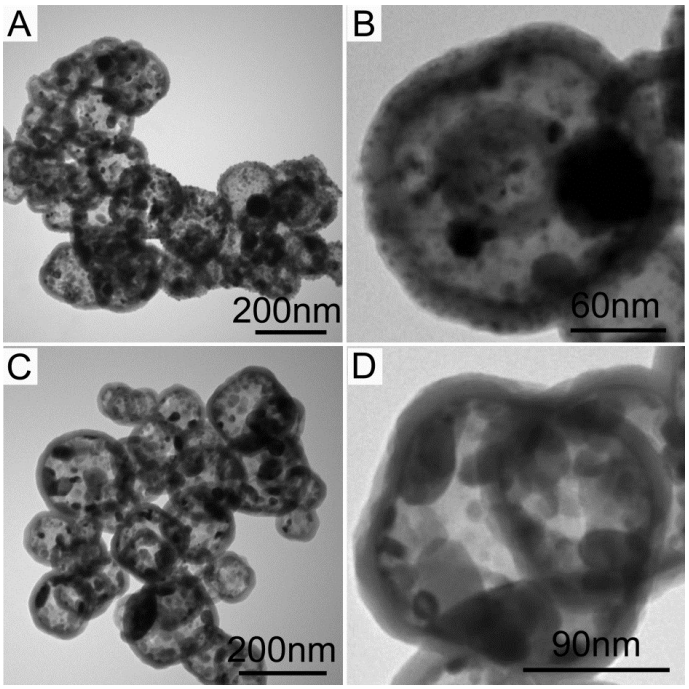

Figure S4. TEM images of (A, B) Co@SiO_2@C/Ni-500, (C,D) Co@SiO_2-500. (0.1 mL of TEOS was used.)

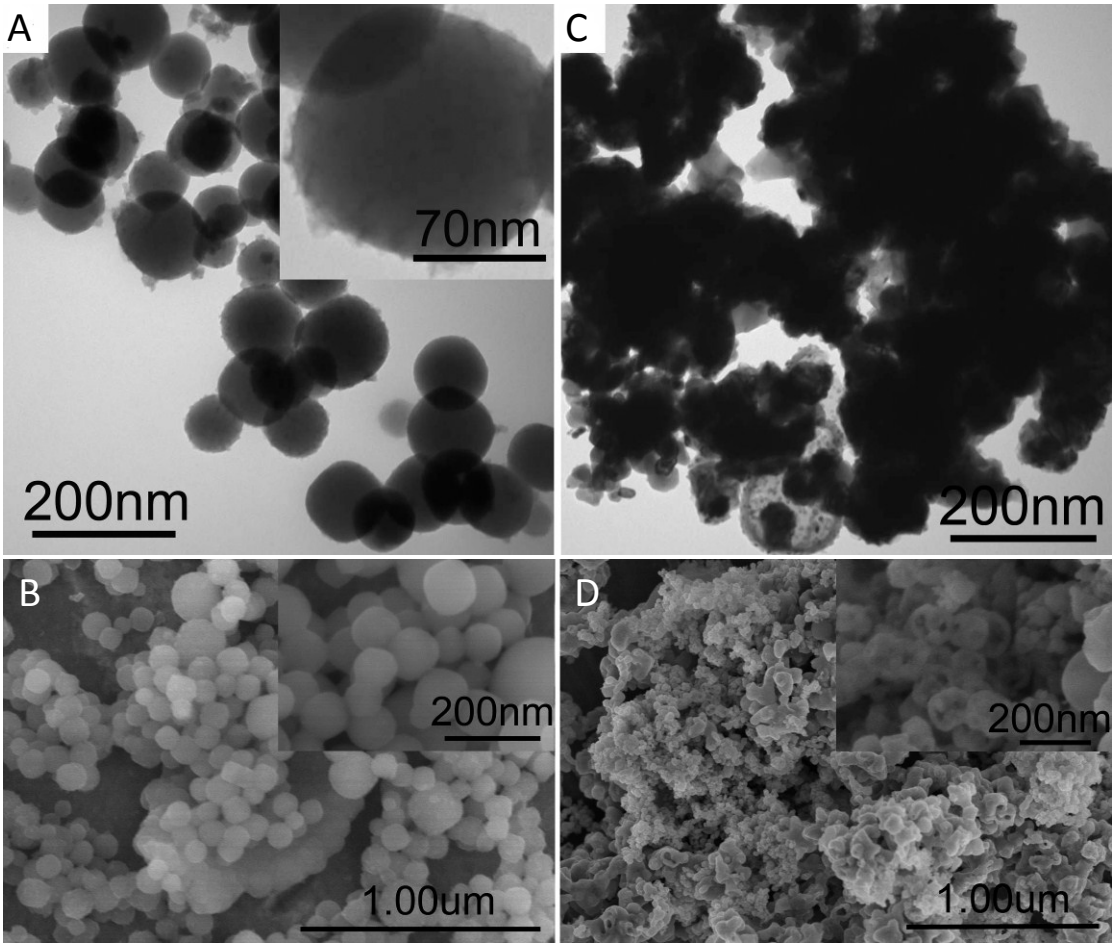

Figure S5. TEM and SEM images of (A,B) $Co_3[Co(CN)_6]_2$@PDA-Ni^{2+}, (C,D) Co-Ni@C composites annealed at 500 °C.

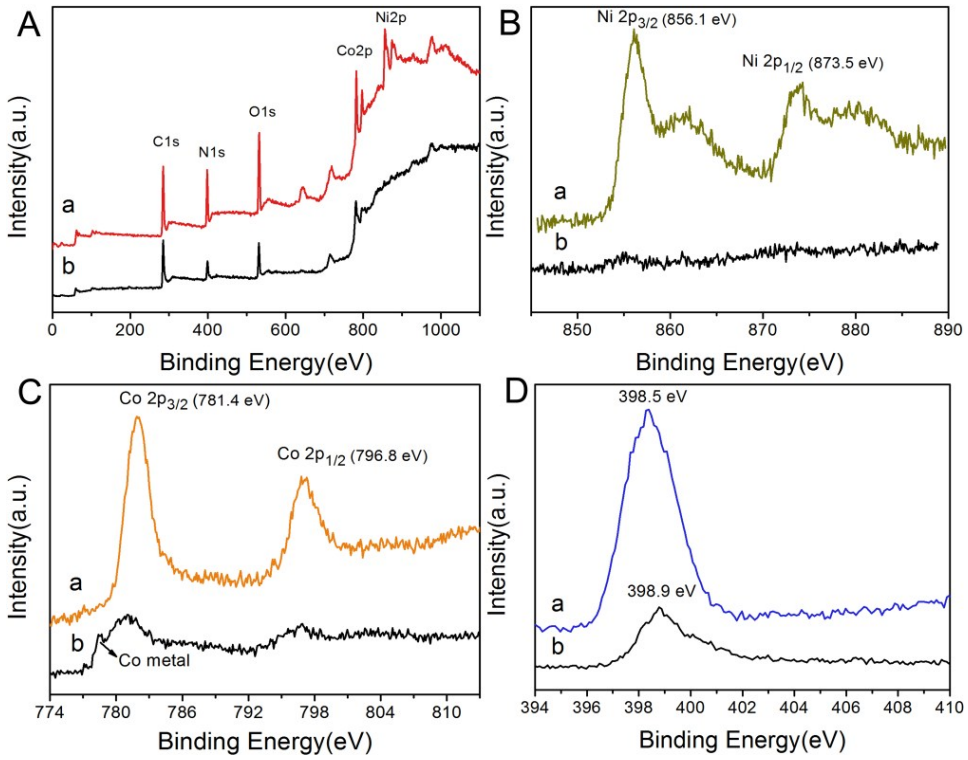

Figure S6. XPS spectra of $Co_3[Co(CN)_6]_2$@PDA-Ni^{2+} composite (a) and Co-Ni@C-500 composite: (A) the full survey scan, (B) Ni 2p, (C) Co 2p, and (D) N 1s.

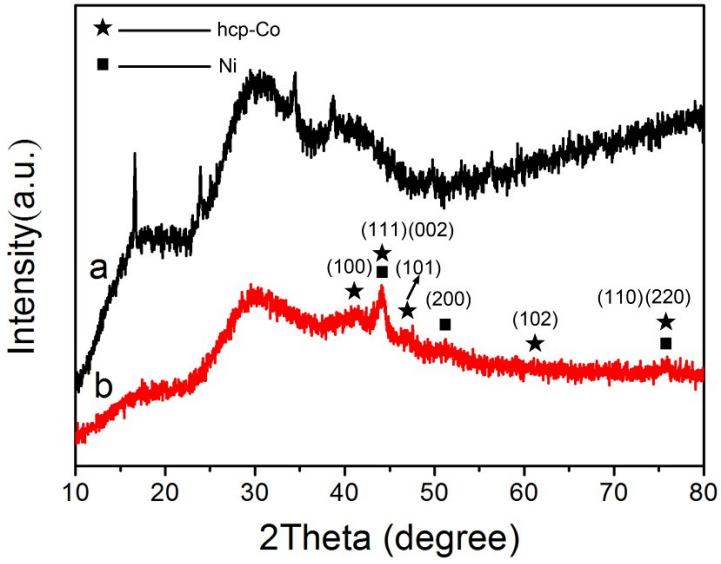

Figure S7. XRD patterns of $Co_3[Co(CN)_6]_2$@PDA-Ni^{2+} (a) and Co-Ni@C-500 (b).

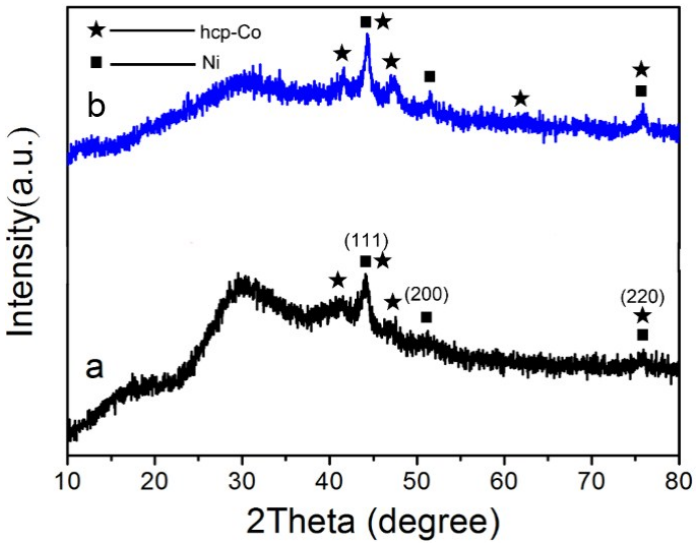

Figure S8. XRD patterns of Co@SiO_2@C/Ni-500 submicrorattles fabricated with the molar ratio of dopamine and nickel ion of 1:0.5 (a) and 1:3 (b).

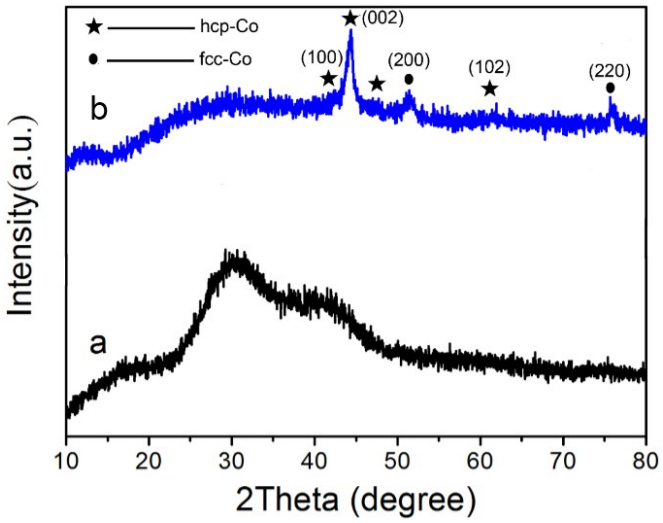

Figure S9. XRD patterns of $Co@SiO_2@C/Ni$ submirorattles annealed at 400 °C (a) and 700 °C (b).

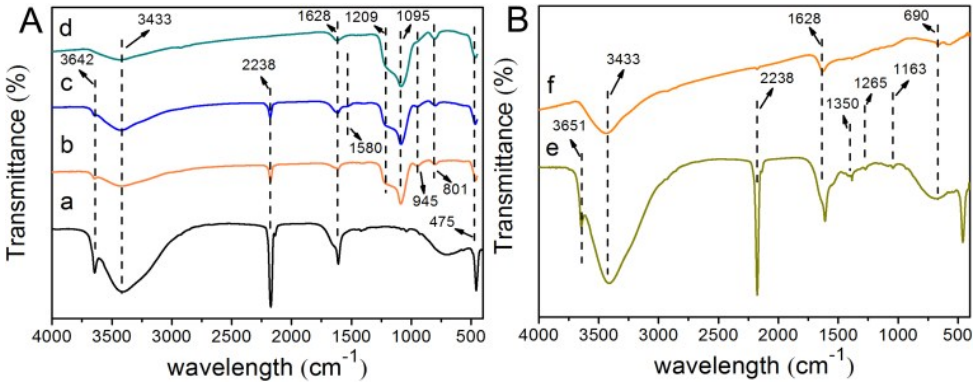

Figure S10. FTIR of $Co_3[Co(CN)_6]_2$ cubes (A), $Co_3[Co(CN)_6]_2@SiO_2$ (B), $Co_3[Co(CN)_6]_2@SiO_2@PDA\text{-}Ni^{2+}$ (C), $Co@SiO_2@C/Ni$-500 submicrorattles (D),

$Co_3[Co(CN)_6]_2$@PDA-Ni^{2+} (E), Co-Ni@C-500 (F).

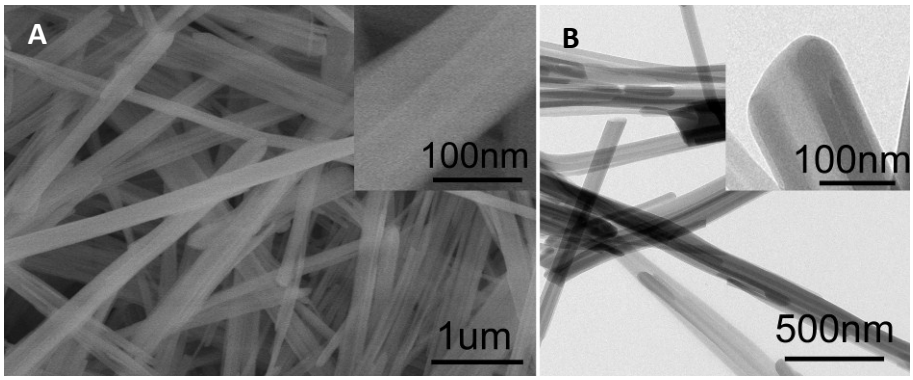

Figure S11. SEM and TEM images of Co-NTC nanowires.

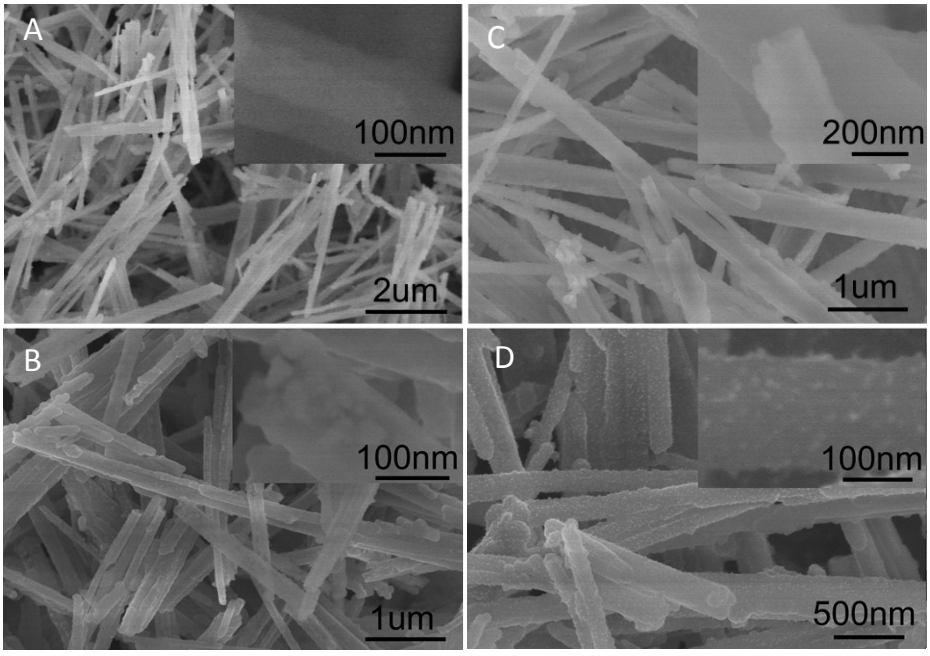

Figure S12. SEM images of (A) Co-NTC@SiO_2, (B) Co@SiO_2 nanocables, (C) Co-

NTC@SiO_2@PDA-Ni^{2+}, (D) Co@SiO_2@C/Ni.

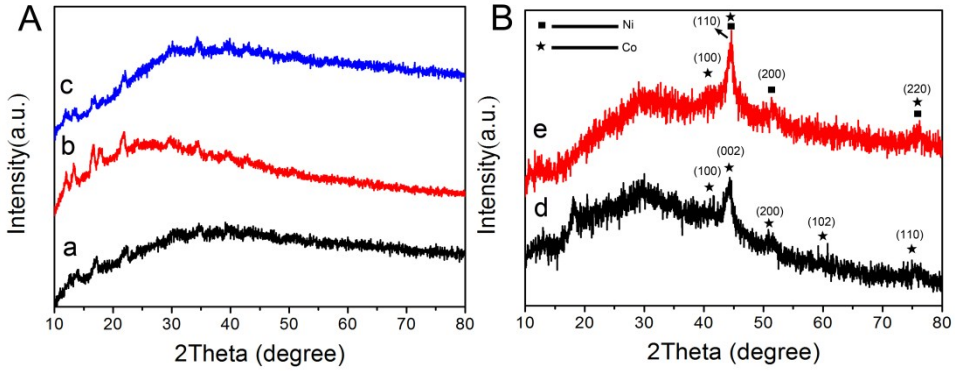

Figure S13. XRD patterns of Co-NTC nanowires (a), Co-NTC@SiO_2 (b), Co-NTC@SiO_2@PDA-Ni^{2+} (c), Co@SiO_2 (d), Co@SiO_2@C/Ni nanotubes (e).

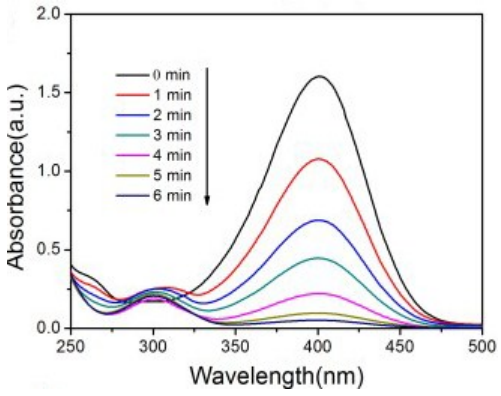

Figure S14. UV-vis absorption spectra of 4-NP at different reaction time during the

reduction by $NaBH_4$ catalyzed by $Co@SiO_2@C/Ni$-700.

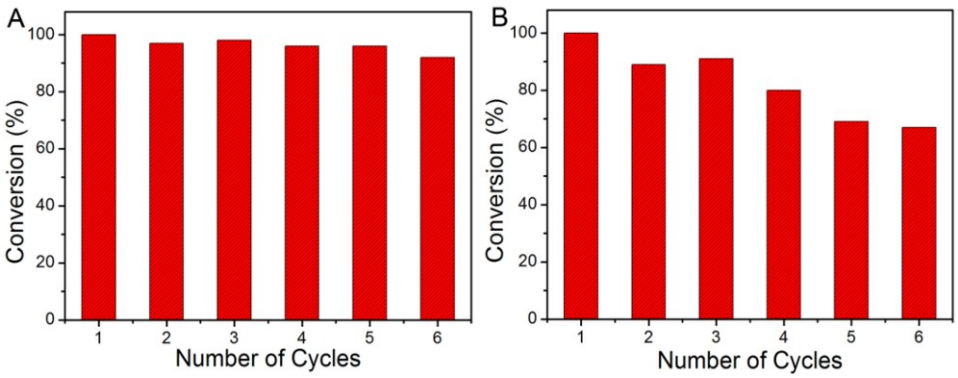

Figure S15. The reusability of $Co@SiO_2@C/Ni$-700 (a) and Co-Ni@C-700 (b) as the catalyst for the reduction of 4-NP with $NaBH_4$.

Table S1. ICP data of $Co@SiO_2$-700, $Co@SiO_2@C/Ni$-700 and Co-Ni@C-700.

Catalyst	Co (μg/mg)	Ni (μg/mg)
$Co@SiO_2$	201.25	/
$Co@SiO_2@C/Ni$	132.25	67.25
Co-Ni@C	417.75	159.75

Table S2. A full comparison of $Co@SiO_2@C/Ni$ submicrorattles catalysis activity and test condition with other cobalt and noble metal catalysts.

Catalyst	K (min^{-1})	κ(mg^{-1} min^{-1})	TOF/h^{-1}	Conversion ratio	Ref.

Co@SiO_2-700	0.38	1.63	27.69	100%	This work
Co@SiO_2@C/Ni-700	0.583	7.74	136.71	100%	This work
Co-Ni@C-500	0.63	1.18	17.82	100%	This work
Au nanoparticles	0.06	0.72	12.13	100%	S1
Pd nanocatalysts	0.732	0.36	6.11	100%	S2
Fe_3O_4@SiO_2-Au@mSiO_2	0.53	6.43	123.76	100%	S3
Au@meso-SiO_2	0.08	2.51	39.02	100%	S4
Ni/SiO_2 (230 nm)	0.504	1.06	18.95	100%	S5
BNNS/Ag-3	0.163	0.96	17.93	100%	S6
Cu_2O-Cu-CuO	0.624	1.242	18.81	100%	S7
P_{PAA}	0.9276	2.306	31.72	100%	S8
Pd/MIL-100(Cr) NCs	1.13	1.506	21.82	100%	S9
Cu_2O@Ag	0.4368	1.094	16.39	100%	S10
Ir/IrOx	0.033	0.71	10.76	100%	S11
2Au@2Ag	0.18	0.632	9.57	100%	S12
reduced Co_3O_4	1.49	2.26	34.23	100%	S13

S1. K. B. Narayanan and N. Sakthivel, *Journal of Hazardous Materials*, 2011, 189, 519-525.

S2. X. Lu, X. Bian, G. Nie, C. Zhang, C. Wang and Y. Wei, *Journal of Materials Chemistry*, 2012, 22, 12723-12730.

S3. Y. Deng, Y. Cai, Z. Sun, J. Liu, C. Liu, J. Wei, W. Li, C. Liu, Y. Wang and D. Zhao, *Journal of the American Chemical Society*, 2010, 132, 8466-8473.

S4. J. Chen, Z. Xue, S. Feng, B. Tu and D. Zhao, *Journal of Colloid and Interface Science*, 2014, 429, 62-67.

S5. Z. Niu, S. Zhang, Y. Sun, S. Gai, F. He, Y. Dai, L. Li and P. Yang, *Dalton Transactions*, 2014, 43, 16911-16918.

S6. H. Shen, C. Duan, J. Guo, N. Zhao and J. Xu, *Journal of Materials Chemistry A*, 2015, 3, 16663-16669.

S7. A. K. Sasmal, S. Dutta and T. Pal, *Dalton Transactions*, 2016, 45, 3139-3150.

S8. C. Kästner and A. F. Thünemann, *Langmuir*, 2016, 32, 7383-7391.

S9. R. Li, Y. Yang, R. Li and Q. Chen, *ACS Applied Materials & Interfaces*, 2015, 7, 6019-6024.

S10. S. Kandula and P. Jeevanandam, *European Journal of Inorganic Chemistry*, 2016, 2016, 1548-1557.

S11. D. Xu, P. Diao, T. Jin, Q. Wu, X. Liu, X. Guo, H. Gong, F. Li, M. Xiang and Y. Ronghai, *ACS Applied Materials & Interfaces*, 2015, 7, 16738-16749.

S12. X. Zhang and Z. Su, *Advanced Materials*, 2012, 24, 4574-4577.

S13. H. Chen, M. Yang, S. Tao and G. Chen, *Applied Catalysis B: Environmental*, 2017, 209, 648-656.